Desalination and Water Treatment
www.deswater.com
doi: 10.1080/19443994.2015.1059372

57 (2016) 13005–13019
June

Taylor & Francis
Taylor & Francis Group

Modeling and optimization by response surface methodology and neural network–genetic algorithm for decolorization of real textile dye effluent using *Pleurotus ostreatus*: a comparison study

M. Venkatesh Prabhu[a,*], R. Karthikeyan[b], M. Shanmugaprakash[c]

[a]*Fermentation Bioengineering Laboratory, Department of Biotechnology, School of Bioengineering, SRM University, Kattankulathur, Chennai 603203, India, Tel. +91 98943 13473; Fax: 044 27453903; emails: venkateshprabhu.m@ktr.srmuniv.ac.in, venkateshlpt@gmail.com*
[b]*Anjalai Ammal Mahalingam Engineering College, Thiruvarur District, Tamil Nadu 614403, India, Tel. 04374 233749; email: drrkarthi@yahoo.com*
[c]*Downstream Processing Laboratory, Department of Biotechnology, Kumaraguru College of Technology, Coimbatore 641049, India, Tel. +91 99423 11658; email: sunbioin@gmail.com*

Received 7 January 2015; Accepted 28 May 2015

ABSTRACT

This study focuses on the modeling and optimization of the decolorization procedure of real textile dye. The percentage of decolorization of effluent in the Erlenmeyer flask level, as obtained by both response surface methodology (RSM) and artificial neural network (ANN), was determined and subjected to comparative evaluation. The effect of independent variables such as pH (5–8), self-immobilized *Pleurotus ostreatus*, bead volume (30–50%) (V_b/V_r), and initial effluent concentration (50–100%) was examined using three-level Box–Behnken design. A similar design was utilized to train a feed-forward multilayered perceptron with back-propagation algorithm. Errors were computed using error functions, and the values obtained for RSM and ANN were compared. The maximum percentage decolorization and COD reduction of effluent under optimized conditions over a 24-h period were observed as 89 and 72%, respectively. The parameters optimized in the flask level were adapted in an inverse fluidized bed bioreactor of 6 l working volume, in which the quantity of decolorization and COD reduction over a 24-h period was observed as 92 and 76%, respectively.

Keywords: Artificial neural network; Response surface methodology; Genetic algorithm; Industrial dye effluent; Inverse fluidized bed bioreactor; *P. ostreatus*

1. Introduction

The bequest of hasty urbanization and industrialization has a corollary in major pollution problems, both in terrestrial and aquatic environments [1]. Textile, cosmetic, food, leather, pharmaceutical, and paper industries consume substantially large amounts of dye [2]. The textile industry, in addition, requires huge amounts of water, energy, and allied chemicals. The daily production of fabric in India averages around 600,000 m. In the process, approximately 1.5 million liters of effluent are formed and discharged without proper treatment, into the surrounding natural water bodies. A total of 20–50% dye remains

*Corresponding author.

in the dye bath in an unfixed hydrolyzed form that has no binding capacity with fabric, thus resulting in colored effluent. Highly colored untreated effluents from the textile industry are a potential environmental hazard if discharged into open water. Rigid environmental regulations are imposed in several countries.

Effluents from the textile industry are of different colors based on market demand. Major pollutants, present in the effluent organic compounds, color, inhibitory compounds, toxicants, pH, salts, chlorinated compounds, and so on, have high BOD, COD, turbidity, TDS, and TSS [2]. Among these, the chief pollutant is color. Upon consideration of the volume and composition of pollutants from various industries, the textile industry is foremost in the discharge of recalcitrant contaminants into the receiving water [3]. This leads to an enragement of the ecological system by a reduction of sunlight penetration and dissolved oxygen concentration. Additionally, dyes are toxic, mutagenic, and a potential source of carcinogenic amines [2,4]. Decolorization by conventional methods is difficult. Physical and chemical engineering methods of remediation such as adsorption, coagulation, and ozonation are prevalent, of which ozonation is complex, requires expensive equipment and chemicals, and is therefore not economically feasible [1]. Biological methods of remediation are efficient, durable, and fiscally viable. A wide range of microorganisms such as bacteria [5–7], fungi [8–10], yeast [11,12], and algae [13–16] may be successfully used for effluent treatment [1]. Biodegradation of dyes by fungus is more advantageous. Lignin-modifying enzymes present in white rot fungus such as lignin peroxidase, manganese peroxidase, and laccase have oxidative bioremediation properties, thereby making the microorganism more suitable for the efficient treatment of textile effluents and dye removal. The active surface area between the enzyme and environment is greater, facilitating rapid conversion of pollutant to nontoxic products [17].

Pleurotus ostreatus, an edible mushroom, was first cultivated in Germany as a means of subsistence during World War II. *P. ostreatus*, a paramount biosorbent, is an economical choice as an efficient decolorizing agent for industrial effluents [18]. Reactors of different types have been developed, to study the decolorization of azo dyes using white rot fungus. It is found that fed batch fluidized bed bioreactor is particularly suitable for orange (II) decolorization [19]. Maximum decolorization of azo dyes has been achieved using immobilized enzymes from *Trametes versicolor* U97 or *Pestalotiopsis* sp. NG007, using a vertical bioreactor system [20].

A majority of the previous reports on the treatment of textile dyes using biological systems involve one-variable-at-a-time (OVAT) on the experimental output, while other parameters remain constant. This makes the process arduous and time consuming. The OVAT method does not provide any information on interaction effect between variables, which is an important determinant of output response in wastewater management. The inability to predict the complete interaction effects between variables is a limitation of conventional methods [21].

Response surface methodology (RSM), a statistical experimental design, has been in use for the last two decades to overcome the limitations of traditional methods and to consider the interactive effect between variables [22]. RSM means to optimize an unknown and noisy function by means of simple function, for a small region under designed experimental conditions. RSM can define the effect of an independent variable either alone or in combination with one or more dependent variables in the process [21,23–27].

A suitable mathematical model has been developed based on the RSM data and is found to be convenient with minimum process knowledge, thereby saving time and experimental cost. However, RSM-based models are accurate only for a limited range of input process parameters, and this limits the usage of RSM models. Treatment of textile effluents is a highly nonlinear process. In order to overcome this limitation, an artificial neural network (ANN) can be applied to develop an empirical model [28,29] for the highly nonlinear process of treatment of textile industry effluents.

ANN, an artificial intelligence algorithm, is an attractive option for modeling complicated and nonlinear systems. ANN can be defined as a group of small elements arranged in parallel that are interconnected with weights. The important characteristic of ANN is learning. There are two modes of operation in ANN: one is training and the other is normal mode. The training mode modifies the parameters of a network, whereas the normal mode applies the trained network(s) for simulating response. In the training phase, the input/output data sets are introduced into the neural network. When the difference between the actual and predicted output values from ANN is calculated, the difference in error can be reduced during the training process by adjusting the weight, till the error has reached the predetermined goal. Experimental design by RSM itself is sufficient to build an effective ANN model. ANN could work better than RSM, since it does not require a prior specification of fitting function. Moreover, it has the potential of universal estimation [21]. To our knowledge, there is

no report available for decolorization of textile dye effluent using inverse fluidized bed bioreactor (IFBBR) by *P. ostreatus*. Therefore, in this study, the decolorization procedure was carried out using Box–Behnken design (BBD) with three factors at three levels. ANN-based models have been developed to predict the relationship between dependent and independent variables. The results predicted by the ANN and RSM techniques were compared by error function measures such as root mean square error (RMSE), mean absolute error (MAE), standard error of prediction (SEP), model predictive error (MPE), chi-square statistic (χ^2), and coefficient of determination (R^2). Evaluation of the results was followed by the optimization of process variables through RSM and ANN–GA. Finally, the efficiency of the entire process was reviewed in order to arrive at the most suitable module for optimum decolorization.

2. Materials and methods

2.1. Sampling, chemicals, and analytical methods

Wastewater from a small-scale industry textile dyeing unit at Kanchipuram district, Tamil Nadu, India, was sampled and characterized, based on its physicochemical features (Table 1). Samples were stored at 4°C to avoid biological activity. All the chemicals used in the study were procured from SRL and Qualigen, India, as analytical reagents. Standard analytical methods were followed [30]. The percentage decolorization of effluent was determined by measuring the absorbance of the sample through UV–vis spectrophotometer (Systronics model No. 2203, India) at 575 nm. Decolorization (%) was calculated using the following equation (Eq. (1)),

Table 1
Physicochemical and biological characteristics of wastewater

Physical examination	Units	Results
Temperature	Celsius	25°C
Color	–	Blackish
Odor	–	Foul
Total dissolved solids	mg/L	1,736
BOD	mg/L	1,200
COD	mg/L	3,768
TSS	mg/L	52
pH	–	6.77
Chromium	mg/L	0.064
Sulfates	mg/L	80
Chlorides	mg/L	425

$$\% \text{ Decolorization} = \left[\frac{A_0 - A_t}{A_0}\right] \times 100 \quad (1)$$

where A_0 is the initial effluent absorbance, A_t is the absorbance at incubation time t. Samples were analyzed for absorbance after centrifuging them at 10,000 rpm for 10 min.

2.2. White rot fungus (WRF)

A hyperlaccase producing white rot fungus *P. ostreatus* 4954 (oyster mushroom) was procured from Microbial Testing and Collection Centre (MTCC), Institute of Microbial Technology (IMTech), Chandigarh, India. The fungus sample was maintained in agar slant with a medium composition of glucose (10 g/l), yeast extract (5 g/l), and agar (15 g/l) at pH 5.8. It was subcultured and grown in a submerged medium encompassing glucose (10 g/l), yeast extract (5 g/l), and salt solution (10 ml/100 ml media) containing KH_2PO_4 (0.2 g/l), $MgSO_4$ (0.05 g/l), $CaCl_2$ (0.01 g/l), and KCl (0.05 g/l). The pH was adjusted to 5.8 using 3 M HCl prior to sterilization (15 psi, 15 min, 121°C). The culture was maintained at 37°C for not less than 8 d in a shaker at 120 rpm to form beads of average diameter 5–10 mm. Viable beads formed through shake flask were utilized for the treatment of real textile dye effluent to study the percentage of decolorization and COD reduction in an IFBBR.

2.3. Inverse fluidized bed bioreactor (IFBBR)

Inverse fluidized bed column is made of borosilicate glass. It comprises four sections—one at the base, two in the middle (test sections), and one at the top. The internal diameter of the bottom-most and test sections is 7.6 cm, and its height is 200 cm. The top section serves as a disengagement section; its internal diameter and height being 13 and 17 cm, respectively. The centrally located test sections are provided with equally spaced pressure tappings, numbering ten in all, which are connected to water-filled manometers. A compressor was used to pump atmospheric air into the ring sparer of diameter 5 cm with perforations of 0.1 mm diameter. Both upper and lower test sections were provided with a mesh, which acted as a support for the packing material or self-immobilized fungal beads. The experimental setup is shown in Fig. 1.

2.4. Experimental design by RSM

A statistical modeling technique named RSM was employed for regression analysis using quantitative

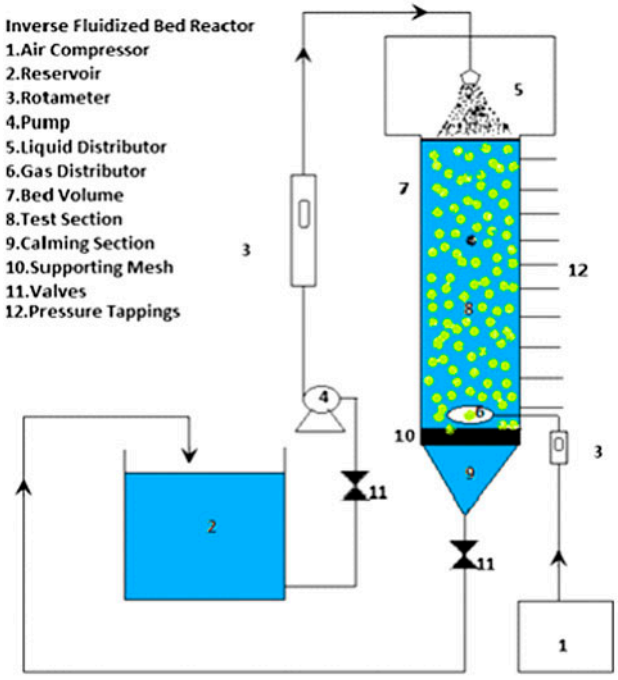

Fig. 1. Schematic diagram of IFBBR.

data obtained through appropriately designed experiments for solving multivariate equations [28]. In this study, BBD with three factors at three levels was applied to evaluate the interactive effect of the variables considered for the decolorization of the effluent. Initial pH (X_1), bead volume (V_b/V_r) % (X_2), (V_b-bead volume and V_r- reactor volume), and initial effluent % (X_3) were selected to study the percentage decolorization (Y) of the industrial effluent sample. Process parameters (coded and uncoded) and their ranges are shown in Table 2.

Second-order polynomial model was developed based on the relationship between response and independent variable. The following equation was used (Eq. (2)),

$$Y = \beta_o + \sum_{j=1}^{k} \beta_i x_i + \sum_{i=1}^{k} \beta_{ii} x_i^2 + \sum_{j=1}^{k-1} \sum_{i>jj=2}^{k} \beta_{ij} x_i x_j + e_i \quad (2)$$

Table 2
Independent variables and its level in BBD

Variables (Units)	Factors	Levels		
	X	−1	0	1
pH	X_1	5	6.5	8
Bead volume (%(V_b/V_r))	X_2	30	40	50
Effluent (%)	X_3	50	75	100

where Y is the decolorization (%), x_i and x_j are the variables (i and j range from 1 to k); β_o is the intercept, β_j, β_{ij} are the interaction of coefficient for laminar, quadratic, and second-order term, respectively, k is the independent parameter ($k = 3$), and e_i is the error.

Adequacy of the model developed was judged by analysis of variance (ANOVA), f-test, and coefficient of determination (R^2). The plots of response surface with contour were developed to examine the relationship between independent and dependent variables. Numerical optimization technique was followed to optimize the independent variable. Statistical analyses was carried out with the help of Stat-Ease Design-Expert Trial version 8.0.7.1 statistical software package (Stat-Ease Inc., Minneapolis, USA) [31].

2.5. Experimental procedure for studies in flask level and IFFBR

Experiments based on BBD matrix were performed in an Erlenmeyer flask as shown in Table 3. Self-immobilized beads of *P. ostreatus* of average diameter 5–10 mm were used for the studies. Bead loading (V_b/V_r), pH, and initial effluent concentration were considered as independent variables, and these were altered according to the design matrix of BBD. Bead volume was considered based on V_b/V_r ratio, where V_r is the reactor holdup volume (100 ml) and V_b is the bead volume, normally 30–50% of V_r. Kinetic studies on the percentage decolorization were conducted at regular time intervals. Optimal conditions were maintained for maximum decolorization. Optimized conditions were validated by performing kinetic studies on both flask level and IFBBR in a completely fluidized state, to accurately measure percentage decolorization and COD reduction. The experiments were duplicated and the mean values were considered for evaluation.

2.6. Modeling by ANN

The ANN model used in the study was similar to the structural and functional aspects of biological neural network. Such a model becomes a powerful tool in the comparative study of the behavior of a new process with an existing one. The basic building blocks of an ANN are constituted by an input layer (independent variable), a number of hidden layers, and an output layer (dependent variables). Each layer consists of inter connected units called neurons. The role of the neuron is to send signals to other neurons with interaction along the weighted connections. The neurons in

Table 3
BBD of independent uncoded variables and their corresponding experimental and predicted values

Run	pH	Bead volume (%(V_b/V_r))	Effluent (%)	% Decolorization		
				Experimental value	Predicted RSM value	Predicted ANN value
1	6.5(0)	40(0)	75(0)	79.10	79.10	79.10
2	6.5(0)	40(0)	75(0)	79.10	79.10	79.10
3	6.5(0)	40(0)	75(0)	79.10	79.10	79.10
4	5(−1)	40(0)	50(−1)	71.30	70.70	70.96
5	6.5(0)	40(0)	75(0)	79.10	79.10	79.10
6	8(+1)	30(−1)	75(0)	70.71	70.11	70.74
7	5(−1)	30(−1)	75(0)	73.15	73.38	73.15
8	5(−1)	40(0)	100(+1)	85.00	84.77	84.98
9	6.5(0)	30(−1)	50(−1)	72.46	72.82	72.55
10	8(+1)	50(+1)	75(0)	73.80	73.57	73.79
11	5(−1)	50(+1)	75(0)	79.13	79.73	79.14
12	6.5(0)	30(−1)	100(+1)	71.62	71.62	71.61
13	6.5(0)	40(0)	75(0)	79.10	79.10	79.10
14	8(+1)	40(0)	50(−1)	73.00	73.24	73.00
15	8(+1)	40(0)	100(+1)	72.20	72.80	72.20
16	6.5(0)	50(+1)	100(+1)	84.90	84.54	84.63
17	6.5(0)	50(+1)	50(−1)	69.71	69.71	69.37

each layer are connected to all other neurons in preceding and following layers through links. The role of the input layer is to get information from the external and convey it to the hidden layer for processing. The individually weighted input values are preprocessed before they enter the hidden layer. The hidden layer processes all data obtained in this manner and produces an output by summing up the modified input values using sigmoidal transfer function.

In this study, tan-sigmoidal transfer function was applied between the input layer and hidden layer and purelin was applied between the hidden layer and outer layer. The network was trained by Levenberg–Marquardt back-propagation algorithm. The factors considered in the RSM were identical to those in the ANN, as was the response (output). The topology of the ANN architecture is illustrated in Fig. 2. The data generated from the experimental design planned through BBD (Table 3) were used to constitute the optimal architecture of ANN. The original dataset (comprising 17 data points) was divided into three subsets, namely 70% training (12 data points), 15% validation (3 data points), and 15% test sets (3 data points). Splitting of data for training, validation, and test subsets was carried out to estimate the performance of the neural network which, in turn, would assist in the prediction of "unseen" data that were unused for training. This step makes possible the assessment of the generality of the ANN model. The

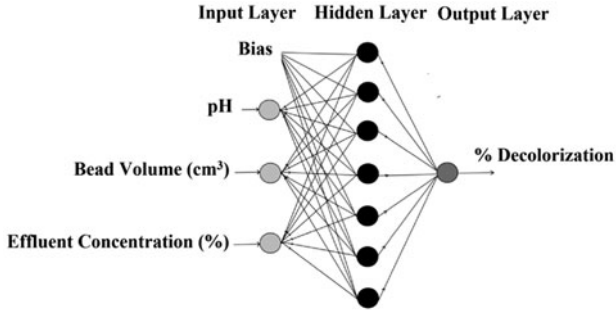

Fig. 2. Schematic diagram of multilayered perceptron neural network.

number of neurons in the hidden layer can be calculated from the expression $2(n + m)^{0.5}$ to $2n + 1$ where n is the number of neurons in the input layer and m the number of neurons in the output layer [32].

With the aim of achieving fast convergence to the minimal RMSE, the inputs and outputs were scaled within the uniform range of −1 (new x_{min}) to 1 (new x_{max}), with the help of the following two equations (Eqs. (3) and (4)), where x_{nor} is the normalized input/output data (data of independent and dependent variables), x_{ac} is the actual variable, and x_{max} and x_{min} are the maximum and minimum values of the particular variable, respectively [33]. This ensured uniform attention during the entire training process.

$$x_{nor} = \frac{2(x_{ac} - x_{min})}{x_{max} - x_{min}} - 1 \quad (3)$$

$$x_{ac} = \frac{(x_{nor} + 1)(x_{max} - x_{min})}{2} + x_{min} \quad (4)$$

All ANN calculations were carried out using Neural Network Toolbox of MATLAB Version 7.9 (R2009b).

2.7. Optimal conditions based on genetic algorithm

Genetic algorithms have been a thriving method for solving both linear and nonlinear problems. It is encouraged by the process of natural selection and genetic evaluation. Mutation, crossover, and selection operations were applied to a population of encoded variable space. The algorithm expands different areas; the parameter space and it searches to the area of high probability of global optimum [34]. GA is used to optimize the input space (X) representing the process variable, with the objective of maximizing the effluent decolorization. The objective of optimization is to ascertain the optimal level of the variable $X^* = [X_1, X_2, X_3]$ and maximize the objective function $f(X^*, w)$ where "w" represents the corresponding weights of the variables and "b" denotes the bias between firstly, input and hidden layer, and secondly, hidden and output layers. The input variables are pH (X_1), bead volume (V_b/V_r) % (X_2), and initial effluent concentration (X_3) with percentage decolorization as the objective. In this study, an ANN model was used as the fitness function for genetic algorithm to optimize the percentage decolorization of effluent [35].

$$\%\ \text{Decolorization} = \text{Purelin}(w2 \times \text{tansig}(w1 \times [X(1); X(2);\ X(3)] + b1) + b2) \quad (5)$$

3. Results and discussion

3.1. RSM model

The results from the studies on the decolorization of textile dye effluent at maximum time according to BBD are presented in Table 3. The quadratic second-order model was formed in terms of coded variables, developed through design expertise, and is given by Eq. (6),

$$\%\ \text{Decolorization} = 79.1 - 2.358X_1 + 2.45X_2 + 3.406X_3 - 0.722X_1X_2 - 3.625X_1X_3 + 4.0075X_2X_3 - 2.1X_1^2 - 2.8025X_2^2 - 1.625X_3^2 \quad (6)$$

where X_1, X_2, and X_3 are the coded values of the given variables.

The ANOVA is a useful tool, in the testing of the significance of the response surface quadratic model. From the ANOVA (Table 4), it is observed that the model was highly significant, the evidence being Fisher's f-value (151.82) with low probability value ($p < 0.0001$). R^2, a correlation coefficient between experimental and predicted value, was checked to find the goodness of fit. The high values of R^2 as 0.9949 indicate that the model was statistically significant and only 0.51% of the variation was not explained by the model. The values of predicted R^2 and adjusted R^2 are 0.9189 and 0.9884, respectively, showing good agreement between the two. A coefficient of variance (CV) of 0.6% proposed better precision and reliability of the data obtained from the experiments. The p-value which is more than 0.05 points to nonsignificant lack of fit which can be interpreted as validity of the model [36]. Hence, ANOVA analysis designates the applicability of the model for the decolorization of textile dye effluent using *P. ostreatus*.

Table 4 shows regression analysis of the model equation on main, square as well as the interaction effects of the independent process variables. p-values less than 0.0001 indicate that the variables are highly significant. Normal % probability graphs (Fig. 3) were used to evaluate the suitability of the model. Results showed that a close relationship exists between the experimental and predicted values. The data lie very close to the diagonal, which represent the proximity of the experimental and simulated data. It is concluded therefore that the developed mathematical model has the ability to describe the decolorization process energetically [31].

3.2. Effect of process variables and its interaction with decolorization

A 3D response surface plot was constructed to investigate the interaction effects of the variables from the developed mathematical models [Fig. 4(A–C)]. From the graph, it is pragmatic that all the combined process variables show significant effect on percentage decolorization [31]. From the plots, it is observed that an increase in pH does not show remarkable changes in the quantity of decolorization and that maximum decolorization was observed between pH 5 and 6. Decolorization percentage increases on increasing bead volume. This could mean that the more the bead volume, the more the active surface area in which dyes can either be biosorbed by the whole cells or degraded by the enzyme laccase. Maximum decolorization was observed at 50% V_b/V_r. It is factual that

Table 4
ANOVA for the experimental results of BBD

Source	Coefficient estimate	Sum of squares	df	Standard error	Mean square	*F*-value	*p*-value	
Model	79.1	373.88	9	0.233	41.542	151.82	<0.0001	Significant
X_1	−2.35	44.509	1	0.184	44.509	162.66	<0.0001	
X_2	2.45	48.02	1	0.184	48.02	175.49	<0.0001	
X_3	3.40	92.820	1	0.184	92.82	339.22	<0.0001	
X_{12}	−0.72	2.0880	1	0.261	2.088	7.6309	0.0280	
X_{13}	−3.62	52.562	1	0.261	52.56	192.09	<0.0001	
X_{23}	4.00	64.240	1	0.261	64.24	234.77	<0.0001	
X_1^2	−2.1	18.568	1	0.254	18.56	67.860	<0.0001	
X_2^2	−2.80	33.069	1	0.254	33.06	120.85	<0.0001	
X_3^2	−1.62	11.118	1	0.254	11.118	40.633	0.0004	

Notes: Residual: 1.92; lack of fit: 1.92; error: 0.00; mean: 76.03; C.V. (%): 0.69; Adeq. precision: 37.529. R^2 = 0.9944; Adj. R^2 = 0.9884; and Pred. R^2 = 0.9185.

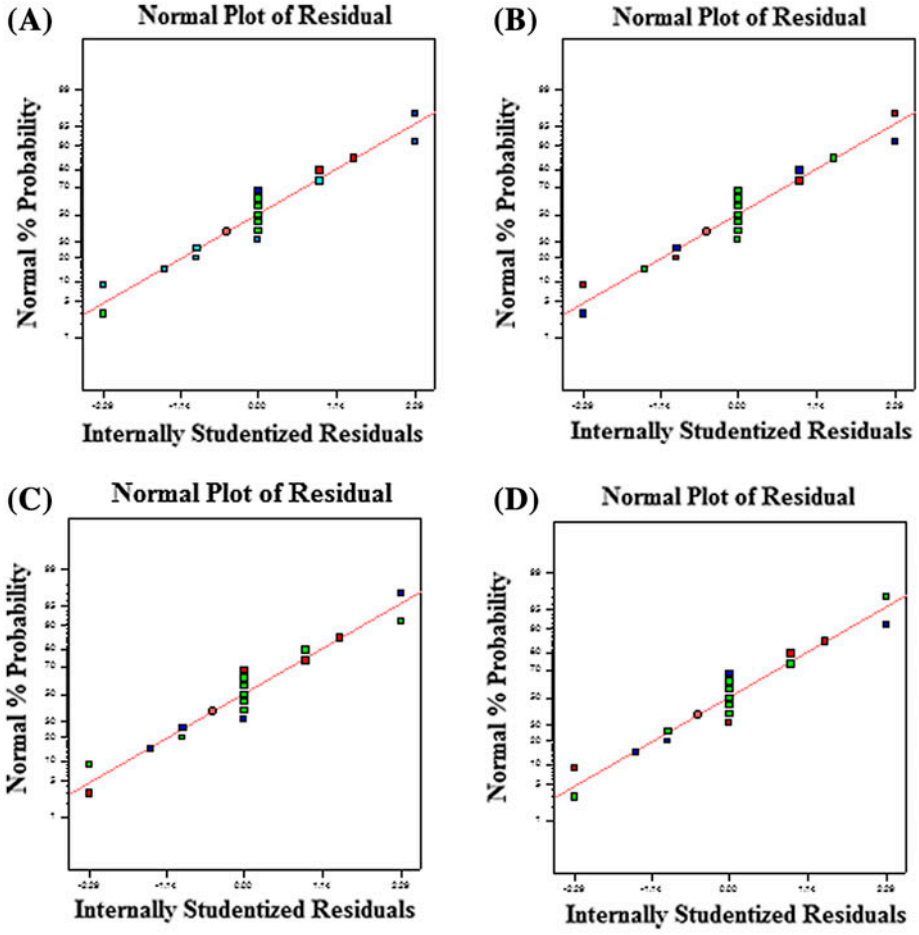

Fig. 3. Normal probability plot of studentized residues for (A) % decolorization; (B) pH; (C) bead volume (*V*/*V* %); and (D) initial effluent concentration.

increase in the initial effluent concentration increases the rate of decolorization, which is predictive of a highly loaded organic pollutant which can either be degraded or biosorbed by the *P. ostreatus* easily. It is evident that *P. ostreatus* shows its potential for application in wastewater treatment.

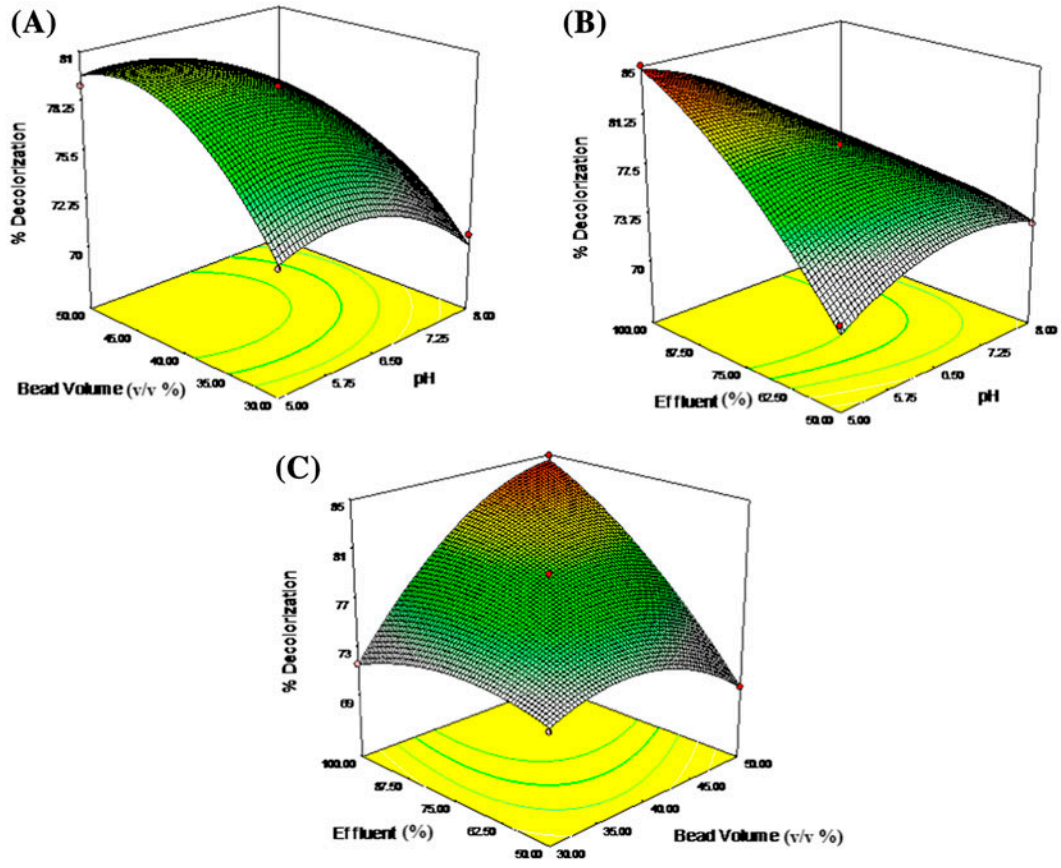

Fig. 4. Three dimensional response surface plot of % decolorization as a function of (A) pH and bead volume (v/v %), (B) pH and effluent %, and (C) bead volume (v/v %) and effluent %.

3.3. ANN model

ANN appears as a powerful tool in the simulation and optimization of processes [37,38]. Therefore, in this study, an ANN-based model was also developed for describing the decolorization of real textile dye effluent. The number of hidden layers and neurons was established in this study by training different feed-forward networks of various topologies and selecting the optimal one, based on minimization of the performance function—mean square error. The resultant optimal architecture (topology) of the ANN model for the present problem involved a feed-forward neural network with one input layer (3 neurons), one hidden layer (7 neurons), and one output layer (1 neuron). This feed-forward network topology is termed as multilayer perceptron, MLP (3:7:1). To comprehend the optimal values of weights and biases, the network MLP (3:7:1) was trained using back-propagation method based on Levenberg–Marquardt algorithm. The model formed through weights and biases is shown in Eq. (7).

$$\begin{aligned}\%\ \text{Decolorization} = {} & -0.821 + (2/((1 + \exp(-2 \times ((X(1) \\ & \times (-1.8806) + X(2) \times 0.56984) + X(3) \\ & \times (1.2593)) - 1) + 3.0459)))) \\ & \times (-0.925) + (2/((1 + \exp(-2 \times ((X(1) \\ & \times (2.6028) + X(2) \times (-1.34141) + X(3) \\ & \times (0.89325)) - 1) + 3.0729)))) \\ & \times (1.0693) + (2/((1 + \exp(-2 \times ((X(1) \\ & \times (-2.3075) + X(2) \times (1.4788) + X(3) \\ & \times (-2.131)) - 1) + 1.7346)))) \\ & \times (0.90149) + (2/((1 + \exp(-2 \\ & \times ((X(1) \times (-1.0822) + X(2) \\ & \times (-1.464) + X(3) \times (-1.9271)) - 1) \\ & - 0.16887)))) \times (-0.56156) + (2/((1 \\ & + \exp(-2 \times ((X(1) \times (0.7455) + X(2) \\ & \times (0.41638) + X(3) \times (2.8893)) - 1) \\ & + 0.32738)))) \times (0.63474) + (2/((1 \\ & + \exp(-2((X(1) \times (0.32565) + X(2) \\ & \times (1.9351) + X(3) \times (2.587)) - 1) \\ & + 1.1976)))) \times (-0.1992) + (2/((1 \\ & + \exp(-2 \times ((X(1) \times (-1.3621) \\ & + X(2)(-0.5908) + X(3)(0.1779)) - 1) \\ & - 2.3015)))) \times (-0.07115)\end{aligned} \tag{7}$$

The plots for the output with respect to training, validation, and test data are given in Fig. 5. The goodness of fit between the experimental and the predicted response given by the ANN model is also shown in Fig. 6. High correlation coefficients indicate the reliability of the developed ANN model. The output follows the targets very well, and the *R*-value is over 0.999. In this case, the network response is satisfactory. On comparing the data predicted by the ANN model with the experimental data, the ANN results are very close to the observed experimental values. The predicted values are in agreement with the experimental values and fall on the diagonal line. Almost all the data fall on this line, confirming the accuracy of the ANN model [39].

3.4. Comparison of RSM and ANN models

The newly constructed ANN and RSM models were compared statistically for their predictive ability. The parameters forming the basis for evaluation included RMSE, SEP (%), MAE, MPE (%), chi-square, and R^2. The models used for error calculation are given in Table 5. Fig. 6 demonstrates clearly that ANN displayed greater predictive ability than RSM. Fig. 7 details residuals between the experimental and the predicted values of RSM and ANN. A close look at the values of error function (Table 6) reveals that the gap between ANN model values and experimental values is extremely narrow. In contrast, RSM model values show a higher error function. It may be inferred that the ANN model is more superior and reliable in its predictive accuracy than RSM when compared with experimental values. These findings therefore firmly establish that ANN may be attributed with the universal ability of approximating nonlinearity of the system [39].

3.5. Optimization by derringers desirability

Attention was given to the following constraints during optimization of the decolorization process of textile dye in the effluent: pH (5–8), bead volume (30–50%) (V_b/V_r), and initial effluent concentration

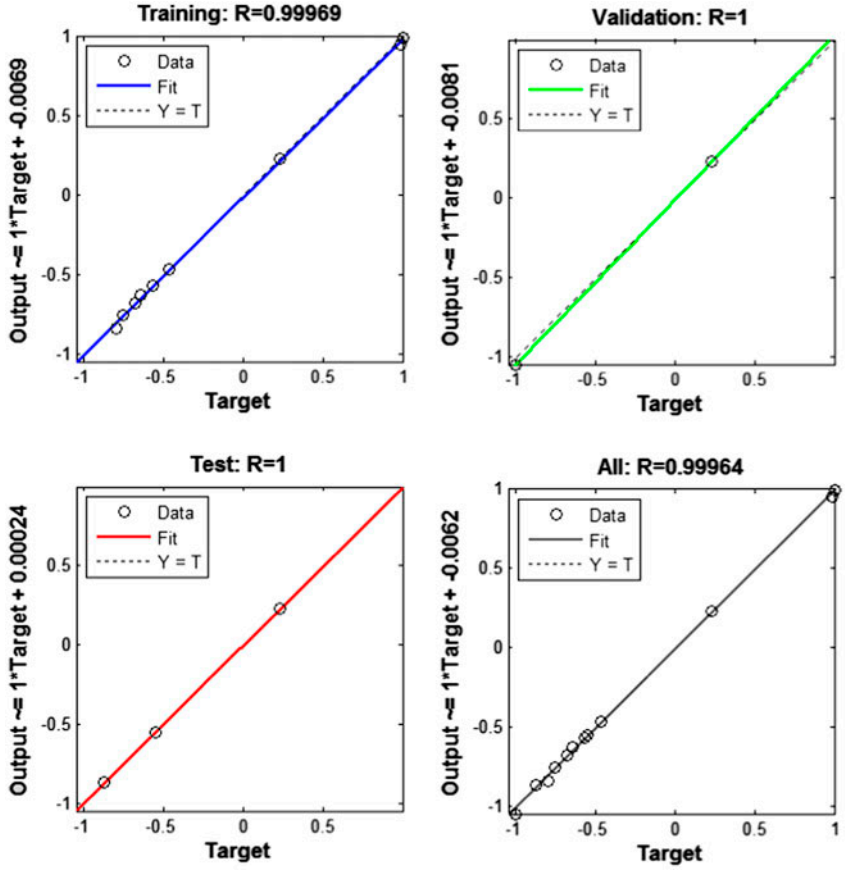

Fig. 5. Neural network model with training, validation, test, and all predicted set for % decolorization.

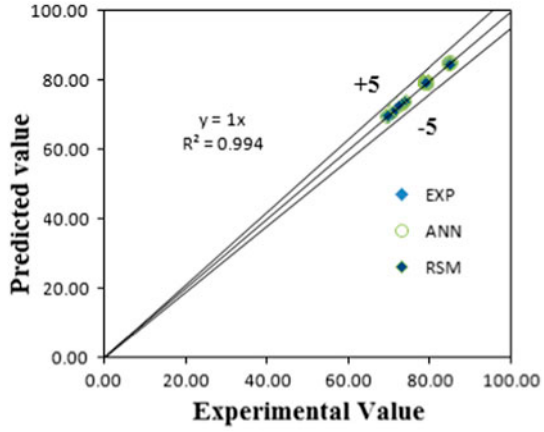

Fig. 6. Comparison of experimental and predicted values of RSM and ANN for % decolorization.

(50–100%); each of which was set for maximum desirability. In numerical optimization, the desired goal was preferred for each variable and response from the menu. The achievable goals were within range (for three independent variables) and maximum (for response only). Applying the methodology of the desired function, optimum levels of process parameters were obtained. The results indicated that maximum decolorization was observed as 88% at pH 5.35, bead volume 50%, and initial effluent concentration of 98.98%. Fig. 8(A) shows a ramp desirability that was developed from optimum points via numerical optimization.

3.6. Optimization by ANN-genetic algorithm

The newly developed ANN model aimed at optimization of process conditions (i.e., input variables) in order to increase percentage decolorization of textile dye. With this objective in mind, genetic algorithms with trained ANN were used as the principal. The optimization problem studied is represented mathematically by:

$$\text{Max net}\begin{pmatrix}\text{pH}\\ \text{Bead volume (v/v)}\\ \text{Int. effluent conc.}\end{pmatrix} = \%\ \text{Decolorization as objective function} \quad (14)$$

$$\text{Bound constraints} = \begin{cases} 5 \le \text{pH} \le 8 \\ 30\% \le \text{Bead volume (v/v)} \le 50\% \\ 50\% \le \text{Int. effluent conc.} \le 100\% \end{cases} \quad (15)$$

Different parameters of GA such as population size, crossover probability value, and mutation probability value were set to be 50, 0.90, and 0.01, respectively. The selection, crossover, and mutation operators were chosen as roulette, heuristic, and uniform methods, respectively. Several GA studies were performed by the authors with different applications [34]. Using ANN as fitness function, optimum solutions were determined after the evaluation of GA operators for 100 iterations to achieve highest possible color removal. The trend in maximum and mean fitness function of response is demonstrated in Fig. 8(B). After successful conversion of responses in neural architecture, the ANN–GA technique evaluated highest percentage decolorization as 89% at pH 5, bead volume 50% (V_b/V_r), and initial effluent concentration of 100% over time 24 h.

3.7. Validation of optimization condition using shakes flask and IFBBR studies

The optimization studies conducted both by derringers desirability function and genetic algorithm were followed for process condition, viz. pH 5, bead volume 50% V_b/V_r, and initial effluent concentration 100%. Decolorization and COD reduction were observed with the above operating conditions at various time intervals. Fig. 9(A) shows percentage decolorization and percentage COD reduction values. It was observed that these two criteria rose to their maximum levels of 89 and 72%, respectively, after 18 h, and thereafter, there was no marked change in the same.

Hydrodynamic studies were conducted for optimizing the operating condition of IFBBR. Bead loading and superficial gas velocity were considered as important operating parameter. It was observed that 30–50% bead volume (V_b/V_r) with density close to water and superficial gas velocity of 0.31 cm/s favoured complete bed expansion in the column, which in turn enhanced the mixing, mass transfer, and contact between the three phases. In this experiment, superficial gas velocity of 0.31 cm/s was taken as operating variable, while the process variables included the conditions optimized by derringers desirability function and genetic algorithm. Percentage decolorization and degradation were observed at constant time interval. Maximum levels for these criteria were found to be 92 and 76%, respectively (Fig. 10(A)). It is inferred that the factors responsible for this phenomenon could be either the laccase enzyme secreted by *P. ostreatus* or surface property of the fungus in the form of greater active surface area of the fungus, resulting in degradation of the dye by the enzyme or its enhanced biosorption.

Table 5
Error functions and its models

Error function	Equation and number	Ref.
Root mean square error	$\mathrm{RMSE} = \sqrt{\frac{1}{n}\sum_{i=1}^{n}\left(Y_{i,e} - Y_{i,p}\right)^2}$ (8)	[41]
Standard error of prediction	$\mathrm{SEP}\ (\%) = \frac{\mathrm{RMSE}}{Y_e} \times 100$ (9)	[42]
Mean absolute error	$\mathrm{MAE} = \frac{1}{n}\sum_{i=1}^{n}\left\lvert Y_{i,e} - Y_{i,p}\right\rvert$ (10)	[42]
Model predictive error (%)	$\mathrm{MPE}\ (\%) = \frac{100}{n}\sum_{i=1}^{n}\left\lvert\frac{Y_{i,e}-Y_{i,p}}{Y_{i,p}}\right\rvert$ (11)	[35]
Chi-square statistics (χ^2)	$\chi^2 = \sum_{i=1}^{n}\frac{\left(Y_{i,p}-Y_{i,e}\right)^2}{Y_{i,p}}$ (12)	[43]
Correlation coefficient (R^2)	$R^2 = 1 - \frac{\sum_{i=1}^{n}(Y_{i,p}-Y_{i,e})}{\sum_{i=1}^{n}(Y_{i,p}-Y_e)^2}$ (13)	[44]

Notes: n is the number of experiments; $Y_{i,e}$ is the experimental value of the ith experiment; Y_{ip} is the predicted value of the ith experiment by model; and Y_e is the average value of experimentally determined.

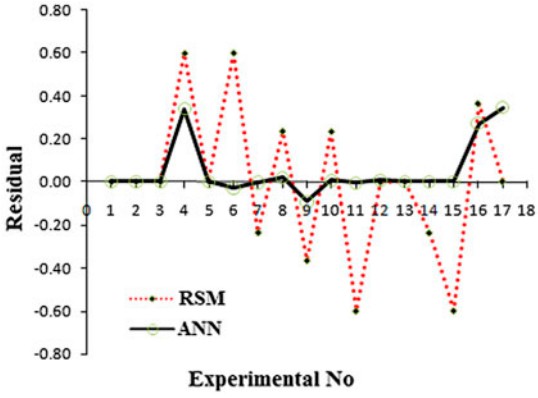

Fig. 7. Distribution of residuals.

Table 6
Error comparisons between RSM and ANN

	% Decolorization	
Statistical parameters	ANN	RSM
RMSE	0.00	0.00
SEP (%)	0.00	0.00
MAE	0.07	0.24
MPE (%)	0.09	0.31
Chi-square	0.0	0.03
R^2	1.00	1.00

The experimental and model output (Figs. 8(A) and 9(A)) states that decolorization and COD reduction of the effluent were growing at the exponential rate up to time interval 18 h, beyond which the rates decreased, probably due to saturation.

3.8. Kinetic studies in Erlenmeyer flask and inverse fluidized bed reactor

The decolorization and degradation kinetics were studied for the treatment of real textile dye effluent under optimized condition of pH, bead volume (V_b/V_r %), and initial effluent concentration, to establish the rate constant. Utilization of the substrate for the decolorization and degradation in both flask and reactor level could biosorb or degrade the contents by the action of *P. ostreatus*. First-order kinetic expression can be used to explain the decolorization and degradation process [40].

$$\frac{dC_s}{dt} = -kC_s \tag{16}$$

C_s is the substrate concentration, t is the time taken for decolorization and degradation in an hour, and k is the rate constant (t^{-1}). Modified first-order studies were conducted to simulate the inverse fluidized bed reactor system, which follows batch reactor [40].

$$\frac{-d(C_s - C_\infty)}{dt} = k(C_s - C_\infty) \tag{17}$$

On integration we get

$$\frac{C_s - C_\infty}{C_0 - C_\infty} = e^{-kt} \tag{18}$$

where C_0 is the initial concentration (mg/l), C_∞, final concentration (mg/l), and k is the pseudo first-order constant (h^{-1}). The concentration of the reactant was

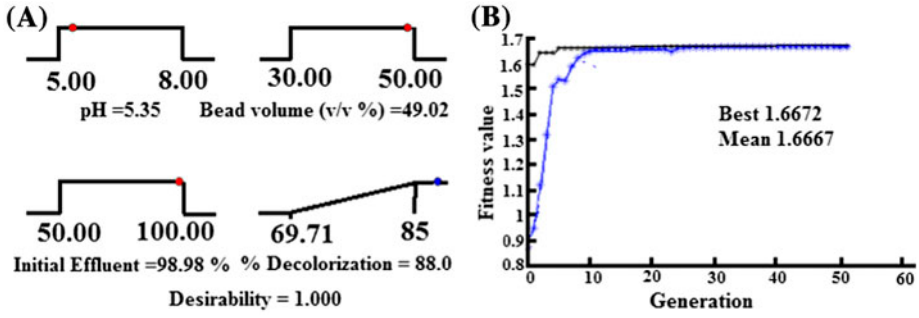

Fig. 8. Optimized desirability ramp (A) derringers desirability ramp and (B) optimization of GA using MATLAB and average fitness value with successive generation showed convergence to optimal value.

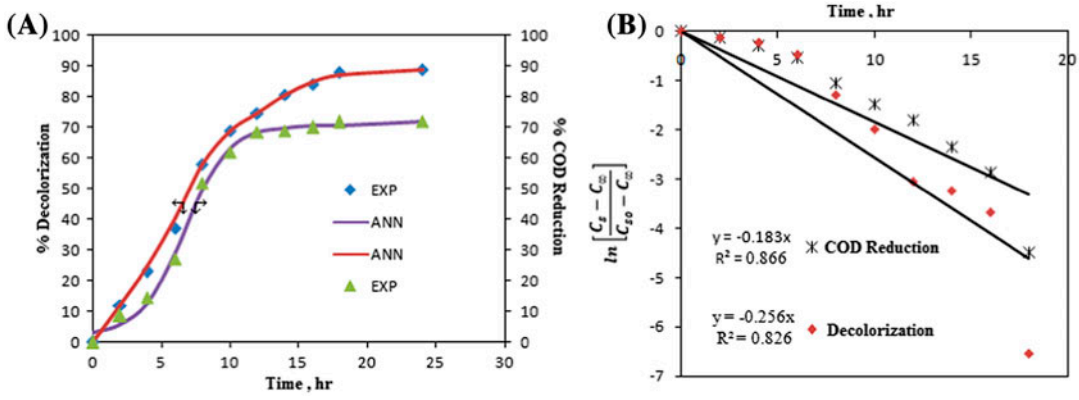

Fig. 9. (A) Performance of Erlenmeyer flask and ability of ANN model to simulate % decolorization and % COD reduction under various operating conditions with respect to contact time. (B) Kinetic study on % decolorization and % COD reduction in Erlenmeyer flask.

reduced gradually by the *P. ostreatus* to become constant after a certain time period: The concentration at that time was C_∞. Experimental data obtained from the flask level and IFBBR were embodied by the above model. The model applied for decolorization and degradation under optimized condition by BBD is shown in Figs. 9(B) and 10(B). A good fit was revealed in the plot between $\ln(C_s - C_\infty)/(C_{so} - C_\infty)$ vs. t. When the R^2 value for levels in the flask (decolorization (0.826) and COD (0.866)) and reactor (decolorization (0.976) and COD (0.947)) were compared, R^2 value for reactor stood better than the flask values. The value of k in both the systems was >0.256 h^{-1}, which is indicative of low activity [40], this could be interpreted as the high substrate concentration possibly causing inhibition of microbial action.

3.9. Sensitivity analysis

As shown in Table 4, the model term of (A) has the largest coefficient (79.1) which suggests that bead volume is the most dominating factor. In comparison with other interactions, this model term has a significant effect on the system. ANN, a black box model, does not give such direct insight into the system. Black box neural network models are allowed to gain the relationships that exist between important variables and are used to predict system variables. Except for a small network, it is almost impractical to expect that the models would easily describe the equations on a short-term basis. It follows that the practical execution of ANNs is difficult. Desai et al. found that ANN is uniformly efficient in sensitivity analysis and interestingly quite comparable to the coefficient of first-order terms in the quadratic RSM equation. However, the nature of the black box for ANN is such that one can perform sensitivity analysis for neural networks with different input variables on the results obtained from the model [32]. There exist numerous methods which describe the procedure for sensitivity analysis of a system using the inherent nature of ANN. Applying Eq. (19), the effect of each input

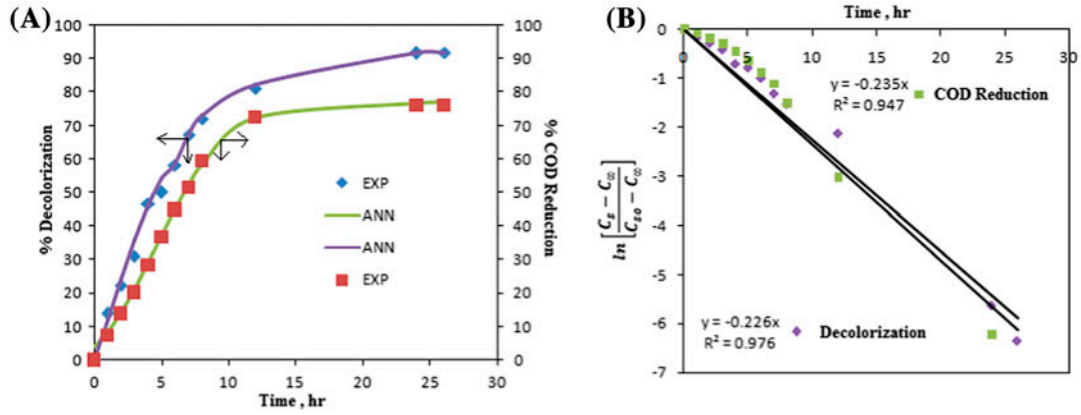

Fig. 10. (A) Performance of IFBBR and ability of ANN model to simulate % decolorization and % COD reduction under various operating conditions with respect to contact time. (B) Kinetic study on % decolorization and % COD reduction in IFBBR.

variable on the output variable modeling matrix was obtained by the network weight

$$I_j = \frac{\sum_{m=1}^{m=N_h}\left(\left(\left|W_{jm}^{ih}\right| / \sum_{k=1}^{N_i}\left|W_{km}^{ih}\right|\right)\times\left|W_{mn}^{ho}\right|\right)}{\sum_{k=1}^{k=N_h}\left\{\sum_{m=1}^{m=N_h}\left(\left|W_{km}^{ih}\right| / \sum_{k=1}^{N_i}\left|W_{km}^{ih}\right|\right)\times\left|W_{mn}^{ho}\right|\right\}} \quad (19)$$

where I_j is the relative importance of the jth input variable on the output variable, N_i and N_h are the numbers of input and hidden neurons, respectively, and Ws are connection weights. The superscripts h and o refer to input, hidden, and output layers, respectively; and subscripts m and n refer to input, hidden, and output neurons, respectively [21]. The relative importance of the input variables and their contribution toward decolorization is 31% by pH. A total of 38% is contributed by initial effluent concentration and rest 31% is by bead volume.

4. Conclusion

Treatment of real textile dye wastewater was carried out using *P. ostreatus* under various operating conditions. It was found that decolorization and degradation of dye effluent was more in IFBBR than in the Erlenmeyer flask level. Maximum levels were attained at 50% V_b/V_r of beads, acidic pH of 5 and at 100% initial effluent concentration, with a COD of 3,768 mg/l. Air flow was continuously maintained at a superficial velocity of 0.31 cm/s. It was observed that maximum decolorization and COD reduction were 89 and 71%, respectively, in flask, and 92 and 76%, respectively, in IFBBR. Kinetic studies showed that both the decolorization and degradation processes adhered to the first-order system. From this study, it may be concluded that RSM can be successfully employed in IFBBR for the management of textile wastewater. Compared to RSM, ANN–GA showed itself to be additionally advantageous for simulation and prediction of experimental results with minimum error. Thus, ANN–GA could be a better alternative than RSM in wastewater treatment.

Acknowledgment

The authors are very grateful to the management of SRM University, Chennai, India, for providing the necessary research facilities, support, and constant encouragement.

References

[1] A. Movafeghi, A.R. Khataee, S. Torbati, M. Zarei, S.Y. Salehi Lisar, Bi removal of C.I. basic red 46 as an azo dye from contaminated water by *Lemna minor* L: Modeling of key factor by neural network, Environ. Prog. 32 (2013) 1082–1089.
[2] F. Deniz, Optimization of biosorption conditions for color removal by Taguchi DOE methodology, Environ. Prog. 32 (2013) 1129–1133.
[3] S. Sandhya, K. Sarayu, K. Swaminathan, Determination of kinetic constants of hybrid textile wastewater treatment system, Bioresour. Technol. 99 (2008) 5793–5797.
[4] S. Torbati, A.R. Khataee, A. Movafeghi, Application of watercress (*Nasturtium officinale* R. Br.) for biotreatment of a textile dye: Investigation of some physiological responses and effects of operational parameters, Chem. Eng. Res. Des. 92 (2014) 1934–1941.
[5] J.P. Jadhav, S.S. Phugare, R.S. Dhanve, S.B. Jadhav, Rapid biodegradation and decolorization of direct orange 39 (orange TGLL) by an isolated bacterium *Pseudomonas aeruginosa* strain BCH, Biodegradation 21 (2010) 453–463.

[6] R.C. Senan, T.E. Abraham, Bioremediation of textile azo dyes by aerobic bacterial consortium aerobic degradation of selected azo dyes by bacterial consortium, Biodegradation 15 (2004) 275–280.
[7] W.D. Constant, J.H. Pardue, R.D. Delaune, K. Blanchard, G.A. Breitenbeck, Enhancement of in situ microbial degradation of chlorinated organic waste at the petro processors superfund site, Environ. Prog. 14 (1995) 51–60.
[8] M.S.M. Annuar, S. Adnan, S. Vikineswary, Y. Chisti, Kinetics and energetics of azo dye decolorization by *Pycnoporus sanguineus*, Water Air Soil Pollut. 202 (2009) 179–188.
[9] A.K. Verma, C. Raghukumar, P. Verma, Y.S. Shouche, C.G. Naik, Four marine-derived fungi for bioremediation of raw textile mill effluents, Biodegradation 21 (2010) 217–233.
[10] R.A. Haimann, Fungal technologies for the treatment of hazardous waste, Environ. Prog. 14 (1995) 201–203.
[11] S.U. Jadhav, S.D. Kalme, S.P. Govindwar, Biodegradation of methyl red by *Galactomyces geotrichum* MTCC 1360, Int. Biodeterior. Biodegrad. 62 (2008) 135–142.
[12] G. Dönmez, Bioaccumulation of the reactive textile dyes by *Candida tropicalis* growing in molasses medium, Enzyme Microb. Technol. 30 (2002) 363–366.
[13] A.R. Khataee, M. Zarei, M. Pourhassan, Bioremediation of malachite green from contaminated water by three microalgae: Neural network modelling, Clean-Soil Air Water 38 (2010) 96–103.
[14] A.R. Khataee, G. Dehghan, A. Ebadi, M. Zarei, M. Pourhassan, Biological treatment of a dye solution by *Macroalgae Chara* sp.: Effect of operational parameters, intermediates identification and artificial neural network modeling, Bioresour. Technol. 101 (2010) 2252–2258.
[15] A.R. Khataee, G. Dehghan, M. Zarei, E. Ebadi, M. Pourhassan, Neural network modeling of biotreatment of triphenylmethane dye solution by a green macroalgae, Chem. Eng Res. Des. 89 (2011) 172–178.
[16] A. Rehman, F.R. Shakoori, A.R. Shakoori, Resistance and uptake of heavy metals by *Vorticella microstoma* and its potential use in industrial wastewater treatment, Environ. Prog. 29 (2010) 481–486.
[17] K. Papadopoulou, I.M. Kalagona, A. Philippoussis, F. Rigas, Optimization of fungal decolorization of azo and anthraquinone dyes via Box-Behnken design, Int. Biodeterior. Biodegrad. 77 (2013) 31–38.
[18] G. Eger, G. Eden, E. Wissig, *Pleurotus ostreatus*? Breeding potential of a new cultivated mushroom, Theor. Appl. Genet. 47 (1976) 155–163.
[19] F.M. Zhang, J.S. Knapp, K.N. Tapley, Development of bioreactor systems for decolorization of orange II using white rot fungus, Enzyme Microb. Technol. 24 (1999) 48–53.
[20] D.H.Y. Yanto, S. Tachibana, K. Itoh, Biodecolorization of textile dyes by immobilized enzymes in a vertical bioreactor system, Proc. Environ. Sci. 20 (2014) 235–244.
[21] P. Pakravan, A. Akhbari, H. Moradi, A.H. Azandaryani, A.M. Mansouri, M. Safari, Process modelling and evaluation of petroleum refinery wastewater treatment through response surface methodology and artificial neural network in a photocatalytic reactor using polyethyleneimine (PEI)/titania (TiO_2) multilayer film on quartz tube, Appl. Petrochem. Res. 5 (2015) 47–59.
[22] G.E. Box, J.S. Hunter, Multi-factor experimental designs for exploring response surfaces, Ann. Math. Stat. 28 (1957) 195–241.
[23] K. Karthikeyan, K. Nanthakumar, K. Shanthi, P. Lakshmanaperumalsamy, Response surface methodology for optimization of culture conditions for dye decolorization by a fungus, *Aspergillus niger* HM11 isolated from dye affected soil, Iran. J. Microbiol. 2 (2010) 213–222.
[24] R.H. Myers, D.C. Montgomery, Response Surface Methodology: Process and Product Optimization using Designed Experiments, Wiley, New York, NY, 1995.
[25] M. Rasouli, S. Seiiedlou, H.R. Ghasemzadeh, H. Nalbandi, Convective drying of garlic (*Allium sativum* L.): Part I: Drying kinetics, mathematical modelling and change in color, AJCS 5 (2011) 1707–1714.
[26] L. Wang, C. Shao, H. Wang, H. Wu, Radial basis function neural networks-based modeling of the membrane separation process: Hydrogen recovery from refinery gases, J. Nat. Gas Chem. 15 (2006) 230–234.
[27] B. Zhao, Y. Su, Artificial neural network-based modeling of pressure drop coefficient for cyclone separators, Chem. Eng. Res. Des. 88 (2010) 606–613.
[28] K.M. Desai, S.A. Survase, P.S. Saudagar, S.S. Lele, R.S. Singhal, R.S. Singhal, Comparison of artificial neural network (ANN) and response surface methodology (RSM) in fermentation media optimization: Case study of fermentative production of scleroglucan, Biochem. Eng. J. 41 (2008) 266–273.
[29] S. Haykin, Neural Networks. A Comprehensive Foundation, Prentice Hall International, New Jersey, NJ, 1998.
[30] A.D. Eaton, M.A.H. Franson, Standard Methods for the Examination of Water and Wastewater, APHA, Washington, DC, 2005.
[31] K. Thirugnanasambandham, V. Sivakumar, J.P. Maran, Efficiency of electrocoagulation method to treat chicken processing industry wastewater—Modeling and optimization, J. Taiwan Inst. Chem. Eng. 45 (2014) 2427–2435.
[32] G.F.S. Valente, R.C.S. Mendonça, J.A.M. Pereira, L.B. Felix, Artificial neural network prediction of chemical oxygen demand in dairy industry effluent treated by electrocoagulation, Sep. Purif. Technol. 132 (2014) 627–633.
[33] M. Shanmugaprakash, V. Sivakumar, Development of experimental design approach and ANN-based models for determination of Cr(VI) ions uptake rate from aqueous solution onto the solid biodiesel waste residue, Bioresour. Technol. 148 (2013) 550–559.
[34] H. Karimi, M. Ghaedi, Application of artificial neural network and genetic algorithm to modeling and optimization of removal of methylene blue using activated carbon, J. Ind. Eng. Chem. 20 (2014) 2471–2476.
[35] M. Zafar, S. Kumar, S. Kumar, A.K. Dhiman, Optimization of polyhydroxybutyrate (PHB) production by *Azohydromonas lata* MTCC 2311 by using genetic algorithm based on artificial neural network and response surface methodology, Biocatal. Agr. Biotechnol. 1 (2012) 70–79.

[36] D.R. Hamsaveni, S.G. Prapulla, S. Divakar, Response surface methodological approach for the synthesis of isobutyl isobutyrate, Process Biochem. 36 (2001) 1103–1109.
[37] K. Sinha, S. Chowdhury, P.D. Saha, S. Datta, Modeling of microwave-assisted extraction of natural dye from seeds of *Bixa orellana* (Annatto) using response surface methodology (RSM) and artificial neural network (ANN), Ind. Crop. Prod. 41 (2013) 165–171.
[38] M.G. Moghaddam, M. Khajeh, Comparison of response surface methodology and artificial neural network in predicting the microwave-assisted extraction procedure to determine zinc in fish muscles, Food Nutr. Sci. 02 (2011) 803–808.
[39] B. Rahmanian, M. Pakizeh, S.A. Mansoori, R. Abedini, Application of experimental design approach and artificial neural network (ANN) for the determination of potential micellar-enhanced ultrafiltration process, J. Hazard. Mater. 187 (2011) 67–74.
[40] S. Sathian, M. Rajasimman, G. Radha, V. Shanmugapriya, C. Karthikeyan, Performance of SBR for the treatment of textile dye wastewater: Optimization and kinetic studies, Alexandria Eng. J. 53 (2014) 417–426.
[41] R.M. García-Gimeno, C. Hervás-Martínez, R. Rodríguez-Pérez, G. Zurera-Cosano, Modelling the growth of *Leuconostoc mesenteroides* by artificial neural networks, Int. J. Food Microbiol. 105 (2005) 317–332.
[42] S. Youssefi, Z. Emam-Djomeh, S.M. Mousavi, Comparison of artificial neural network (ANN) and response surface methodology (RSM) in the prediction of quality parameters of spray-dried pomegranate juice, Drying Technol. 27 (2009) 910–917.
[43] A. Çelekli, F. Geyik, Artificial neural networks (ANN) approach for modeling of removal of Lanaset Red G on *Chara contraria*, Bioresour. Technol. 102 (2011) 5634–5638.
[44] M. Rajendra, P.C. Jena, H. Raheman, Prediction of optimized pretreatment process parameters for biodiesel production using ANN and GA, Fuel 88 (2009) 868–875.